J. Phys. B: At. Mol. Opt. Phys. 25 (1992) 199-211. Printed in the UK

Electron capture by protons and alpha particles from two-electron targets

Yu Rang Kuang

China Center of Advanced Science and Technology (World Laboratory), PO Box 8730, 100080, People's Republic of China
and
Physics Department, Chengdu University of Science and Technology, Chengdu, Sichuan 610065, People's Republic of China†

Received 26 July 1991

Abstract. The modified two-orthogonal state expansion method published recently is applied to calculate electron capture cross sections for two-electron systems: H^+, $He^{2+}+Be^{2+}$, B^{3+}, C^{4+}, N^{5+} and O^{6+}, $H^+ + He$ and $He^{2+} + Li(1s^2)$. The active electron is described by the independent-electron model. The calculated results agree well with the existing experimental data for $H^+ + He$ and $He^{2+} + Li$ collisions in the ranges 5-130 keV and below 500 keV amu^{-1} respectively. Our results for H^+, $He^{2+} + C^{4+}$ systems are in good agreement with the experimental values for H^+, $He^{2+} + CH_4$ collisions in the intermediate energy range. A comparison with other theoretical results is presented. Scaling laws for these cross sections are examined.

1. Introduction

In a previous paper (Kuang 1991a, herafter referred to as I) a new modified two-orthogonal state expansion method was developed and has been applied to calculate the capture cross section of the electron by protons and α particles in collision with single-electron ionic targets (Kuang 1991a, b). The calculated results show very good agreement with the experimental data at intermediate energies. In this paper, we shall directly apply this method to calculate the capture cross sections for the following collisions

$$H^+, He^{2+} + A^{(Z-2)+} - H(1s), He^+(1s) + A^{(Z-1)+} \tag{1}$$

$$H^+ + He(1s^2) - H(1s) + He^+(1s) \tag{2}$$

$$He^{2+} + Li(1s^2 2s) - He^+(1s) + Li^+(1s2s) \tag{3}$$

where $A^{(Z-2)+}$ and $A^{(Z-1)+}$ respectively indicate the helium-like and the hydrogenic ions for atoms Be, B, C, N and O. The above reactions are very interesting in thermonuclear fusion research. Many reports deal with reactions (2) and (3). For reaction (1), no research has been reported except for $H^+ + Li^+$ collisions. In I, we performed calculations for the $H^+ + Li^+$ system and the results are in good agreement with the experimental data (Sewell *et al* 1980).

The notation used here is the same as in I.

† Address for correspondence.

0953-4075/92/010199+13$04.50

2. Method

The method used here has been reported in I and will not be repeated. Now we only outline the following several points. First, we think about the physical model adopted in I. A projectile Z_p with impact velocity v and impact parameter b collides with a hydrogenic target of charge Z_t (figure 1). In the initial channel, i.e. before transfer, the Coulomb field of the projectile will distort the initial electronic wavefunction. In our model, a united atom is used to express this effect. The charge of the united atom is optimized by the variational principle in order to ensure that the active electron is always in the ground state of the united atom before transfer. For the initial 1s electron, the charge determined variationally is

$$Z = Z_t + Z_p(1+2ZR)\,e^{-2ZR} \tag{4}$$

which automatically changes from the separated-atom limit (Z_t) to the united-atom limit (Z_t+Z_p). In the meantime, the effective charge Z ensures that the electronic wavefunction

$$U_j(\boldsymbol{r}_1, \boldsymbol{R}) = \pi^{-1/2} Z^{3/2}\, e^{-Zr_1} \tag{5}$$

consistently changes from that of the separate atom ($R \to \infty$) to that of the united atom ($R \to 0$), which overcomes the difficulty that the general atomic orbital expansion will produce an unphysical property at small R.

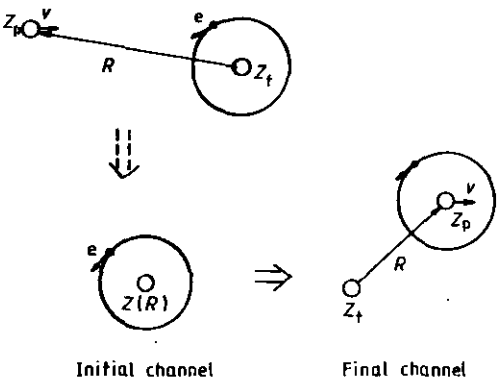

Figure 1. Collision scheme.

Notice that the present variational principle is slightly different from that used by Cheshire (1968) and McCarroll *et al* (1970) where the effective charge is related to the projectile velocity (see equations (27) and (19) in the papers of Cheshire (1968) and McCarroll *et al* (1970) respectively). So the variational principle is invalid unless the impact velocity is very low. However, the present method, as mentioned above, will not have this trouble.

In the final channel, i.e. after transfer, a pure hydrogenic wavefunction centred on the projectile is used in I. Strictly speaking, the distortion of the final wavefunction by the residual target ion should be considered. This effect will reduce the capture

cross section because the residual ion pulls the electron back. However, the final united-atom effect will increase the capture probability because of the bigger effective charge of the projectile. That is, the final distortion should not be expressed by the united atom. The correct treatment is to adopt the logarithm phase factor distortion (Decker and Eichler 1989, Belkic *et al* 1986, Belkic 1988). But the above effect is not too important for collisions at intermediate energies.

Next, it is very interesting to discuss the 'orthogonalized factor' $D_j(R)$ in I. From (17) in I, the factor $D_j(R)$ reads

$$D_j(R) = Z(Z - Z_t) - \frac{Z_p}{R}[1 + (1 + ZR)\,e^{-2ZR}] \tag{6}$$

which really comes from

$$D_j = \left\langle U_j(\boldsymbol{r}_1, \boldsymbol{R}) \left| \frac{Z - Z_t}{r_1} - \frac{Z_p}{r_2} \right| U_j(\boldsymbol{r}_1, \boldsymbol{R}) \right\rangle. \tag{7}$$

Namely, it is an averaged initial residual potential. Hence the initial average energy (7) in I may be written as

$$E_j = -\tfrac{1}{2}Z^2 + D_j(R). \tag{8}$$

From (7) and (8), the factor $D_j(R)$ should vanish at both asymptotic regions, i.e. at small and large R. It is not difficult to see that the expression (6) meets these asymptotic conditions, which is a direct result of the initial united-atom effect. If we do not adopt the united-atom model in the initial channel (Bates 1958), the initial energy (8) is incorrect at small R because the Hamiltonian has an exact hydrogen-like eigenfunction with charge $Z_t + Z_p$ and an eigenvalue $\frac{1}{2}(Z_t + Z_p)^2$ as $R \to 0$. In figure 2, the factors $D_j(R)$ with and without the united-atom effect are plotted as a function of the nuclear separation R for $H^+ + He$ system (using the independent electron model for He and the effective charge $Z_t = 1.6875$). This figure shows that both curves agree well with each other at large R but their behaviours are very different at small R. The curve without the united-atom effect tends to a constant $-Z_pZ_t$ as $R \to 0$. The incorrect behaviour of $D_j(R)$ without the united-atom effect at small R will lead to bigger effects for calculations of the capture cross section. In addition, the reason why the factor

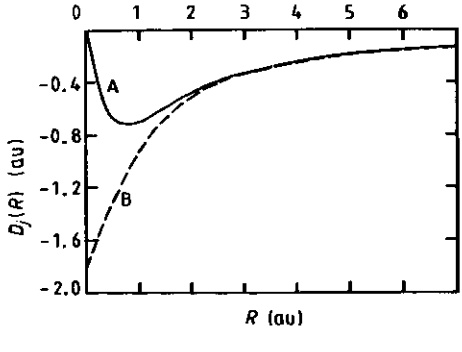

Figure 2. The orthogonalized factor $D_j(R)$ is plotted as a function of the nuclear separation R. Curves A and B correspond to the factors with and without the initial united-atom effect respectively.

$D_j(R)$ is called the orthogonalized one is that it comes from orthogonalization treatment between the initial and the final wavefunctions for collision process.

3. Results

3.1. Two-electron ion systems

In I, we used the independent-electron model to describe two-electron ion Li^+. In this model, the active electron 'sees' an effective charge which reproduces the experimental ionization potential: $Z_t = (2E_i)^{1/2}$ which is called the binding energy screening charge (BES). Here we still adopt the independent-electron approximation for two-electron ions Be^{2+}, B^{3+}, C^{4+}, N^{5+} and O^{6+}. The BES charges for these ions are 3.364, 4.342, 5.370, 6.372 and 7.373, respectively. The present calculations for collisions H^+ and $He^{2+} + Be^{2+}$, B^{3+}, C^{4+}, N^{5+} and O^{6+} are given in tables 1 and 2 and plotted in figures 3 and 4, respectively. The impact energy extends from 20 to 2000 keV amu^{-1}.

Table 1. The calculated 1s–1s capture cross sections for H^+–Be^{2+}, B^{3+}, C^{4+}, N^{5+} and O^{6+} collisions. Units are cm^2.

E (keV)	$Be^{2+}(10^{-18})$	$B^{3+}(10^{-19})$	$C^{4+}(10^{-20})$	$N^{5+}(10^{-20})$	$O^{6+}(10^{-21})$
20	0.050				
30	0.146				
40	0.286	0.108			
50	0.451	0.202			
75	0.868	0.546	0.388	0.0402	
100	1.18	0.971	0.816	0.0948	0.134
125	1.36	1.40	1.41	0.175	0.267
150	1.42	1.80	2.03	0.280	0.450
175	1.41	2.11	2.71	0.402	0.688
200	1.34	2.34	3.36	0.541	0.972
250	1.14	2.60	4.54	0.832	1.65
300	0.935	2.62	5.41	1.11	2.42
400	0.585	2.30	6.25	1.60	4.03
500	0.368	1.84	6.26	1.88	5.45
750	0.124	0.925	4.62	1.94	7.25
1000	0.0488	0.466	3.05	1.59	7.31
1250		0.245	1.92	1.20	6.37
1500		0.135	1.22	0.847	5.28
1750		0.0790	0.800	0.631	4.21
2000			0.530	0.455	3.30

From figures 3 and 4, it can be seen that the present theoretical curves for 1s–1s capture show the same shape and a peak exists at some impact energy. The peaks appear at about 165, 290, 450, 650 and 900 keV for $H^+ + Be^{2+}$, B^{3+}, C^{4+}, N^{5+} and O^{6+}, and at 95, 200, 390, 600 and 810 keV amu^{-1} for $He^{2+} + Be^{2+}$, B^{3+}, C^{4+}, N^{5+} and O^{6+}, respectively. According to the Oppenheimer–Brinkman–Kramers approximation (OBK), the position of the peak should appear at the following energy

$$E = \tfrac{25}{6} Z_t^2 \{s - 2 + [(s-2)^2 + 24s^2]^{1/2}\} \tag{9}$$

Table 2. As table 1 but for He^{2+} projectiles.

E (keV amu^{-1})	$Be^{2+}(10^{-17})$	$B^{3+}(10^{-18})$	$C^{4+}(10^{-18})$	$N^{5+}(10^{-19})$	$O^{6+}(10^{-19})$
20	0.966				
30	1.77	0.499			
40	2.44	0.966			
50	2.90	1.54	0.0828		
75	3.38	3.02	0.225	0.222	
100	3.33	4.35	0.414	0.475	0.066
125	3.05	5.30	0.621	0.810	0.122
150	2.71	5.89	0.824	1.20	0.196
175	2.39	6.17	1.00	1.63	0.247
200	2.06	6.31	1.16	2.06	0.398
250	1.56	6.05	1.38	2.91	0.616
300	1.19	5.48	1.52	3.62	0.851
400	0.711	4.25	1.54	4.64	1.29
500	0.444	3.17	1.42	5.05	1.63
750	0.159	1.52	0.955	4.66	1.93
1000	0.068	0.767	0.586	3.60	1.82
1250		0.421	0.378	2.62	1.53
1500		0.242	0.243	1.89	1.24
1750		0.146	0.160	1.37	0.982
2000		0.092	0.106	1.00	0.764

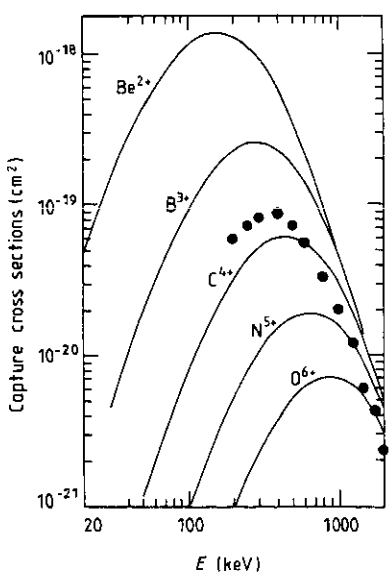

Figure 3. 1s–1s capture cross sections for $H^+ + Be^{2+}$, B^{3+}, C^{4+}, N^{5+} and O^{6+} collisions. The full curves are the present calculations. The experimental values are taken from the results of Rodbro *et al* (1979) for $H^+ + CH_4$ collisions.

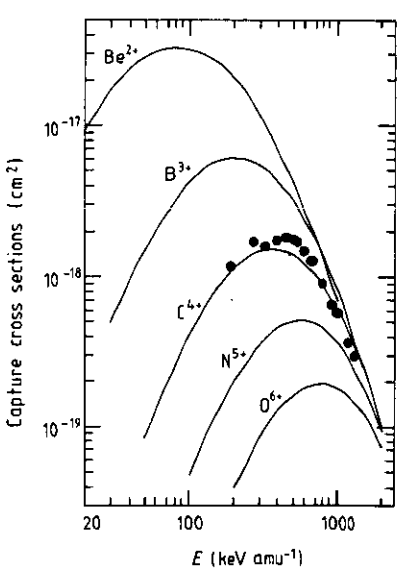

Figure 4. Similar to figure 3 for He^{2+} projectiles.

where $s = 1 - Z_p^2/Z_t^2$ and the unit of energy is keV amu^{-1}. It may be checked that the above peak positions for all systems calculated here are in good agreement with ones predicted by OBK.

No experimental data are available for the above colliding systems except for indirect results for H^+ and $He^{2+} + CH_4$ collisions (Rodbro *et al* 1979). Because four outer-shell electrons of carbon pair up with ones of four hydrogen atoms and the capture mainly comes from the K-shell of C atom in the energy range calculated here, the projectiles will see an ion just like $C^{4+}(1s^2)$. Figures 3 and 4 show that the present K–K cross sections are in generally good agreement with the experimental data (capture into all discrete states of the projectiles) in the intermediate energy region, especially for He^{2+} projectile where the screening effect of the passive electrons is ignorable because of strong Coulomb field of the projectile.

3.2. Reaction $H^+ + He$

For the He atom, two kinds of effective charge 'seen' by the active electron may be chosen: the Slater screening charge (ss) $Z_t = 1.6875$ (Bransden and Sin Fai Lam 1966, Deco *et al* 1984, Avakov *et al* 1990) and the BES charge $Z_t = 1.345$ (Suzuki *et al* 1984). Many experiments show that a maximum of the capture cross section appears at about 25 keV (Williams and Dunbar 1966, Stedeford and Hasted 1955, Rudd *et al* 1983, Shah and Gilbody 1985, Shah *et al* 1989). According to the OBK prediction (9), the effective charge should be the ss value $Z_t = 1.6875$. Using the ss charge, we calculate the 1s–1s cross sections for $H^+ + He$ collision. The results are presented in table 3 and plotted

Table 3. 1s–1s cross sections for $H^+ + He$ collisions. Units are 10^{-16} cm^2. Experimental total cross sections: a, Shah *et al* (1989); b, Shah and Gilbody (1985); c, Rudd *et al* (1983).

		Experiments $H(\Sigma)$		
E (keV)	This work H(1s)	a	b	c
1	0.0689			
3	0.133			
5	0.370			0.372
7	0.626			0.692
9	0.850			
11	1.02	1.13 ± 0.06		
13	1.15	1.42 ± 0.07		
16	1.27	1.58 ± 0.07		
19	1.33	1.69 ± 0.08		
23	1.33	1.85 ± 0.08		
28	1.26	1.71 ± 0.08		
34	1.15	1.44 ± 0.07		
40	1.02	1.28 ± 0.06		
48	0.858	1.01 ± 0.05		
58	0.689	0.80 ± 0.05		
70	0.528	0.595 ± 0.03		0.675
84	0.394	0.40 ± 0.03		
100	0.284	0.274 ± 0.014		0.287
130	0.162		0.14 ± 0.02	
160	0.0977		0.0752 ± 0.011	
200	0.0533		0.0365 ± 0.004	

in figure 5. The proton energy extends from 1 to 200 keV. This figure shows that the present results are in reasonable agreement with the experimental findings in the energy range 5–130 keV. Our theoretical values are about 25% lower than very recent experimental data (Shah *et al* 1989) near the peak. But it should be noticed that a factor of up to 30% to allow for capture into excited states (Mapleton 1961) is added to the present values in order to compare with the experimental data, which will make our results in better agreement with experiments.

The four atomic orbital expansion (AO4) (Sin Fai Lam 1967) shows a similar shape of the capture curve to ours, but his values overestimate the present results and the experimental data in the full energy region calculated here. However, it is surprising that both results reach a good agreement as proton energy goes down to 1 keV and goes up to 100 keV. In the meantime, the two atomic orbital expansion (AO2) (Bransden and Sin Fai Lam 1966) accord well with the AO4 data. So it is obvious that the use of the initial united-atom in the present two orthogonal state expansion method has greatly improved the results of the AO2 and the AO4 approximations at intermediate energies. The results of the molecular orbital approach (MO) (Kimura 1985) show a better agreement with observed data on the lower side, but they begin to deviate from the recent data (Shah *et al* 1989) above 30 keV if the excited state captures are added. The results, obtained by using the united atomic-orbital-molecular-orbital matching method (AO–MO) (Kimura and Lin 1986), are about 10% higher than the MO values

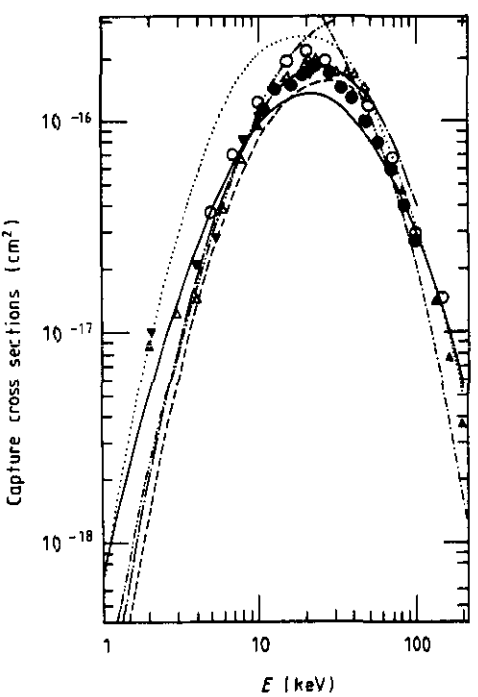

Figure 5. 1s–1s capture cross sections for $H^+ + He$ collisions. Theory: ——, this work; · · · ·, AO4 (Sin Fai Lam 1967); – · · –, low velocity theory (Hughes and Crothers 1977); – – –, MO (Kimura 1985); — · —, AO–MO (Kimura and Lin 1986); – · –, the corrected first Born approximation (Belkic 1988). Experiment: ▲, Shah and Gilbody (1985); ●, Shah *et al* (1989); ○, Rudd *et al* (1983); ▼, Stedeford and Hasted (1955); △, Williams and Dunbar (1966).

above 4 keV and higher than the experiments above 30 keV. The low velocity theory (Hughes and Crothers 1977) is valid below 10 keV. However, the corrected-boundary first Born approximation (Belkic 1988) well describes the collision process above 50 keV.

3.3. Reaction $He^{2+}+Li$

A lithium atom contains three electrons. At low impact energies, the transition electron is mainly the 2s one. The K-shell electron becomes more important when the projectile energy goes up to about 50 keV amu^{-1} and the capture dominantly comes from the K electrons above that energy. The outer 2s electron only leads to a small effect for $He^{2+}+Li$ collisions. However, the situation is very different for the $H^{+}+Li$ system where the outer electron screening becomes very important, which can be seen by comparing the data for $H^{+}+Li^{+}$ (Sewell *et al* 1980) with those for $H^{+}+Li$ (Shah *et al* 1985). The reason is that the Coulomb field of the proton is much weaker than that of the alpha particle. Namely, the present method is valid for $He^{2+}+Li$ collisions if we consider a lithium atom as a two-electron ion Li^{+}. The effective charge 'seen' by the active electron, as in the case of He, is chosen to be the SS one $Z_t=2.6875$. At the same time, we also calculate the cross sections for the BES charge $Z_t=2.184$. The calculated K–K capture cross sections are presented in table 4 and plotted in figure 6. In order to compare with experimental values, total cross sections captured into all

Table 4. The K-shell capture cross sections for He^{2+}–Li collision. The SS and BES columns correspond to results obtained by using the SS and the BES effective potentials. The unit is 10^{-17} cm^2.

E (keV amu^{-1})	SS		BES		
	σ_{1s-1s}	σ_{total}[a]	σ_{1s-1s}	σ_{total}[a]	$\sigma_{exp}(\Sigma)$[b]
10	11.8	11.8	103.0		
15	15.8	15.8	71.7		
22	17.7	17.7	49.9		160 ± 14
29	17.5	17.5	37.2		61.5 ± 3.1
40	15.8	15.8	25.7		21.9 ± 1.4
55	13.2	13.2	17.3		12.2 ± 0.8
63	11.9	11.9	14.5		10.9 ± 0.4
75	10.2	10.2	11.4		9.39 ± 0.62
108	6.89	7.58	6.63	7.29	6.84 ± 0.44
127	5.56	6.12	5.09	5.60	5.63 ± 0.35
150	4.41	4.85	3.83	4.21	4.58 ± 0.30
180	3.30	3.63	2.73	3.00	3.57 ± 0.30
210	2.54	3.05	2.02	2.42	3.02 ± 0.19
250	1.84	2.21	1.40	1.68	2.16 ± 0.14
300	1.27		0.94	1.31	1.45 ± 0.10
350	0.91		0.65	0.91	0.86 ± 0.06
410	0.63		0.43	0.60	0.586 ± 0.042
473	0.44		0.29	0.41	0.352 ± 0.026
547	0.30		0.20	0.28	0.225 ± 0.014

[a] Obtained by multiplying σ_{1s-1s} by 1.0, 1.1, 1.2 and 1.4 at energies below 100, 100–200, 200–300 and above 300 keV amu^{-1} respectively.

[b] The experimental data are taken from the results of Shah and Gilbody (1985). These data are sum of the K- and L-shell contributions of the lithium atom.

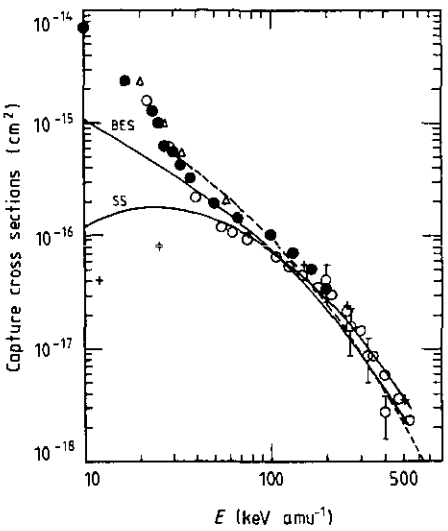

Figure 6. The K-K capture cross sections for He^{2+} + Li collision. Theory: ——, SS, BES, the present SS and BES calculations; – – –, the corrected first Born approximation (Belkic 1989); +, the AO43 results (Ermolaev *et al* 1987). Experiment (sum of the K- and L-shell capture): ○, Shah and Gilbody (1985); ●, McCullough *et al* (1982); △, DuBois and Toburen (1985); ◇, Sasao *et al* (1986).

discrete states, as a reference, are presented in the entry σ_{total} of that table. They are obtained by multiplying the σ_{1s-1s} values by 1.0, 1.1, 1.2 and 1.4 at energy intervals below 100, 100–200, 200–300 and above 300 keV amu^{-1} respectively, according to the results of Ermolaev *et al* (1987), Saha *et al* (1986) and Belkic (1987, 1989). Taking into account about 15% experimental error, we believe that the above estimates do not lead to too large a deviation. It can be seen from table 4 and figure 6 that the present SS capture cross sections are in excellent agreement with the experimental values (McCullough *et al* 1982, DuBois and Toburen 1985, Shah and Gilbody 1985) at energies below 300 keV amu^{-1}, taking into account the extra contribution from excited states. For example, the estimated SS total cross sections are 10.2, 4.85, 3.05 and 2.21×10^{-17} cm^2 to be compared with the experimental data 9.36 ± 0.62, 4.58 ± 0.30, 3.02 ± 0.19 and $2.16 \pm 0.14 \times 10^{-17}$ cm^2 at energies 75, 150, 210 and 250 keV amu^{-1} respectively (Shah and Gilbody 1985). Above 300 keV amu^{-1} our SS cross sections will lie above the observed data because of about 30% capture into excited states of He^+. The figure also shows that the capture from the L shell of the Li atom begins to become important below 60 keV amu^{-1}. The K-shell capture slowly changes in that interval and a peak appears at about 30 keV amu^{-1}. So the present SS calculations can explain the 'shoulder' of the experimental curve at about 50 keV amu^{-1} (McCullough *et al* 1982, Dubois and Toburen 1985, Shah and Gilbody 1985).

On the other hand, our BES results agree well with the observed data above 100 keV amu^{-1} and with the SS results within the experimental errors at energies 100–250 keV amu^{-1}. But the BES values show better behaviour at high energies. For example, the total BES cross sections (table 4) are 1.31, 0.91, 0.60 and 0.41×10^{-17} cm^2 to be compared with the experimental values 1.45 ± 0.10, 0.86 ± 0.06, 0.586 ± 0.042 and $0.352 \pm 0.026 \times 10^{-17}$ cm^2 at energies 300, 350, 410 and 473 keV amu^{-1} respectively (Shah and Gilbody 1985). Above 500 keV amu^{-1}, the BES results also lie above the observed

data. Compared with the ss values, the BES results show very large capture cross sections at low energies which disagree with the experiments.

The 43-state atomic orbital expansion method (AO43) (Ermolaev *et al* 1987) shows very good agreement with the ss calculation at 75 keV amu^{-1}, the former is 10.7×10^{-17} cm^2 and the latter is 10.2×10^{-17} cm^2. However, the AO43 results lie above the present ss values in the interval 100–500 keV amu^{-1}. The maximum difference of 25% appears at 150 keV amu^{-1}. In addition, both results show a slight discrepancy on the lower energy side. The maximum of the capture cross section appears at about 30 and 50 keV amu^{-1} for the ss and the AO43 calculations respectively. It is obvious that the corrected first Born approximation (Belkic 1989) shows very good agreement with experiments and the BES curve over 200 keV amu^{-1}, but the former indicates a slightly more divergent trend in the lower energy side. The calculations of Decker and Eichler (1989) are similar to those of Belkic in the energy region calculated here.

3.4. Probabilities

The normalized probabilities times impact parameter $bP(b)/\sigma$ plotted against impact parameter are shown in figures 7, 8 and 9. Figures 7 and 8 correspond to projectiles

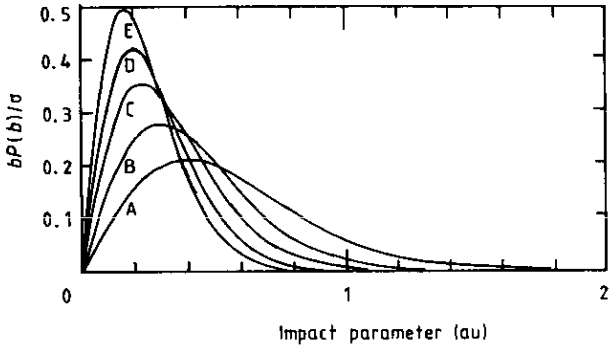

Figure 7. Normalized probabilities times parameter $bP(b)\sigma$ plotted against impact parameter b for 1s–1s electron capture for $H^+ + Be^{2+}$, B^{3+}, C^{4+}, N^{5+} and O^{6+} collisions at peak energies $E = 165$, 290, 450, 650 and 900 keV, labelled by A, B, C, D and E, respectively. The area under each curve is $(2\pi)^{-1}$.

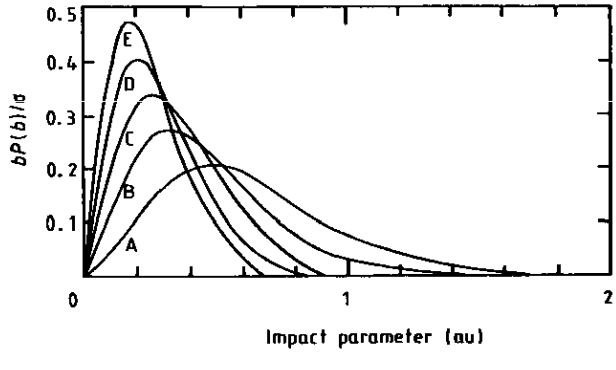

Figure 8. Similar to figure 7 for He^{2+} projectiles at peak energies $E = 95$, 200, 390, 600 and 810 keV amu^{-1} respectively.

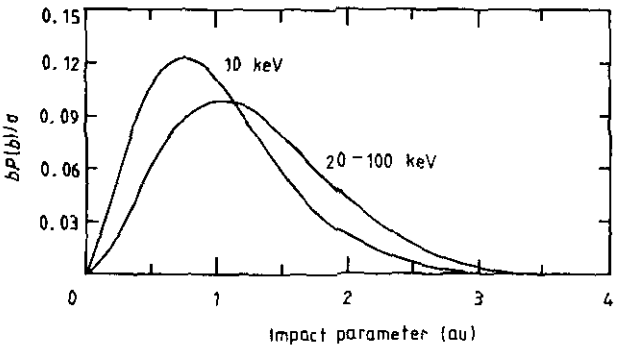

Figure 9. Similar to figure 7 for $H^+ + He$ collision at energies 10 and 20–100 keV.

H^+ and He^{2+} and figure 9 to the reaction $H^+ + He$. In figures 7 and 8, the energy chosen for each curve is the peak energy of that reaction where the capture cross section reaches a maximum. An approximate $1/Z_t$ dependence in the position of the peak, as in other reports (Winter 1987, Kuang 1991b), is observed in figures 7 and 8 respectively. The positions of the peak for the same target but different projectile are slightly different. For proton projectiles, the peak impact parameter B_p is nearly equal to $1.25/Z_t$. But for alpha particle projectiles, it is $1.42/Z_t$. The $bP(b)$ curves for $H^+ + He$ collisions (figure 9) are all single-peak ones in the full energy range calculated here. The locations of the peak are nearly stationary at 1.0 a_0 at energies 20–100 keV and less than 1.0 a_0 out of that range. The AO-MO calculations show that the $bP(b)$ curves are two-peaked below 40 keV and single peaked above that energy (Kimura and Lin 1986). It is interesting to note that the locations of the main peak in the AO-MO approximation are less than 1.5 a_0 below 10 keV and larger than 1.5 a_0 above 20 keV. We think that because the initial united-atom effect makes the active electron closer to the target nucleus, the peak impact parameter becomes smaller and the two peaks are depressed into the single peak.

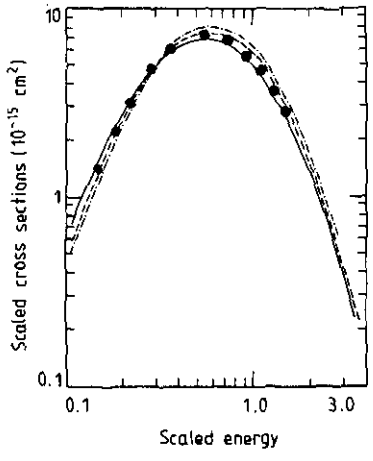

Figure 10. Scaled capture cross sections are plotted as a function of scaled energy. ——, $H^+ + Be^{2+}$; – – –, $H^+ + B^{3+}$; – · –, $H^+ + C^{4+}$; ●, $He^{2+} + O^{6+}$.

3.5. Scaling laws

In the OBK theory, the scaled cross section $\sigma Z_t^7/Z_p^5$ against scaled energy $E/(25Z_t^2\ \text{amu})$ should be a universal curve if $Z_p \ll Z_t$. In figure 10, the scaled cross section is plotted as a function of the scaled energy. The curves for $H^+ + N^{5+}$ and O^{6+} collisions are not shown because these curves almost coincide with the curve of the $H^+ + C^{4+}$ system. For He^{2+}-helium-like systems, we only plot the curve for the O^{6+} ion target for which the above condition $Z_p \ll Z_t$ is satisfied. From figure 10, it is seen that the calculated results obey the OBK scaling laws.

4. Conclusions

So far, the method developed by considering the initial united-atom effect has been applied to calculate 1s–1s capture cross sections for one-and two-electron systems. The calculations show good agreement with the experiments and other theories at intermediate energies. We think that further studies should include the distortion of the final wavefunction so as to improve its high energy behaviour.

Acknowledgment

I wish to thank the Editorial Board of *J. Phys. B: At. Mol. Opt. Phys.* for sending some material helpful in the preparation of this paper.

References

Avakov G V, Ashurov A R, Blokhintsev L D, Kadyrov A S, Mukhamedzhanov A M and Poletayeva M V 1990 *J. Phys. B: At. Mol. Opt. Phys.* **23** 4151
Bates D R 1958 *Proc. R. Soc.* A **247** 294
Belkic Dž 1987 *Phys. Rev.* A **35** 1991
—— 1988 *Phys. Rev.* A **37** 55
—— 1989 *Phys. Scr.* **40** 610
Belkic Dž, Gayet R, Hanssen J and Salin A 1986 *J. Phys. B: At. Mol. Phys.* **19** 2945
Bransden B H and Sin Fai Lam L T 1966 *Proc. Phys. Soc.* **87** 653
Cheshire I M 1968 *J. Phys. B: At. Mol. Phys.* **1** 428
Decker F and Eichler J 1989 *Phys. Rev.* A **39** 1530
Deco G R, Maidagan J M and Rivarola R D 1984 *J. Phys. B: At. Mol. Phys.* **17** L707
DuBois R D and Toburen L H 1985 *Phys. Rev.* A **31** 3603
Ermolaev A M, Hewitt R N and McDowell M R C 1987 *J. Phys. B: At. Mol. Phys.* **20** 3125
Hughes J G and Crothers D S F 1977 *J. Phys. B: At. Mol. Phys.* **10** L605
Kimura M 1985 *Phys. Rev.* A **31** 2185
Kimura M and Lin C D 1986 *Phys. Rev.* A **34** 176
Kuang Y R 1991a *J. Phys. B: At. Mol. Opt. Phys.* **24** 1645
—— 1991b *J. Phys. B: At. Mol. Opt. Phys.* **24** L103
Mapleton R A 1961 *Phys. Rev.* **122** 528
McCarroll R, Piacentini R D and Salin A 1970 *J. Phys. B: At. Mol. Phys.* **3** 137
McCullough R W, Goffe T V, Shah M B, Lennon N and Gilbody H B 1982 *J. Phys. B: At. Mol. Phys.* **15** 111
Rodbro M, Horsdal Pedersen E, Cocke C L and Macdonald J R 1979 *Phys. Rev.* A **19** 1936
Rudd M E, DuBois R D, Toburen L H, Ratcliffe C A and Goffe T V 1983 *Phys. Rev.* A **28** 3244
Saha G C, Datta S and Mukherjee S C 1986 *Phys. Rev.* A **34** 2809
Sasao M, Sato K, Matsumoto A, Amemiya S, Masuda T, Tsurita Y, Fukiza F, Haruyama Y and Kanamori Y 1986 *J. Phys. Soc. Japan* **55** 102
Sewell E C, Angel G C, Dunn K F and Gilbody H B 1980 *J. Phys. B: At. Mol. Phys.* **13** 2269

Shah M B and Gilbody H B 1985 *J. Phys. B: At. Mol. Phys.* **18** 899
Shah M B, McCallion P and Gilbody H B 1989 *J. Phys. B: At. Mol. Opt. Phys.* **22** 3037
Sin Fai Lam L T 1967 *Proc. Phys. Soc.* **92** 67
Stedeford J B H and Hasted J B 1955 *Proc. R. Soc.* A **227** 466
Suzuki H, Kajikawa Y, Toshima N, Ryufuku H and Watanabe T 1984 *Phys. Rev.* A **29** 525
Williams J F and Dunbar D N 1966 *Phys. Rev.* **149** 62
Winter T G 1987 *Phys. Rev.* A **35** 3799